JCTLM DB Extent-of-equivalence study for NML (LGC) (UK) and NIM China reference measurement procedures (RMPs) for *KRAS* p.G12D/WT DNA quantification: NML/LGC report

Dates of analysis: 30.06.2022 Gravimetric dilutions
30.06.2022 dPCR experiment 1
01.07.2022 dPCR experiment 2
04.07.2022 dPCR experiment 3

Analyst: Ana Fernandez-Gonzalez
Science Leader: Alison Devonshire
Internal review: Alexandra Whale/Alison Woolford

Background

A bilateral extent-of-equivalence study was organised by NIM China (NIMC) and the National Measurement Laboratory hosted at LGC (NML/LGC) to compare the performance of NML/LGC's reference measurement procedure (RMP) (Whale *et al*., 2018: JCTLM DB identification number: C15RMP1) and NIMC's nominated RMP (Dong *et al.*, 2018). There are some differences in the measurands and scope of the two RMPs (Table 1), however as variant/wild-type (WT) copy number concentration and variant allelic frequency (vAF) are intrinsically linked, feedback from the JCTLM DB Cycle 18 review process was that an extent-of-equivalence study should be performed to inform the review team and potential users of the RMPs.

Table 1: Overview of NML/LGC and NIMC RMPs for *KRAS* p.G12D/WT

RMP	**NML/LGC**	**NIMC**
Measurand(s)	*KRAS* p.G12D copy number concentration *KRAS* wild-type (p.G12) copy number concentration	*KRAS* p.G12D vAF
Scope	Validated for linearised/digested plasmid or gene fragment materials in an aqueous solution or non-mammalian carrier DNA. This method is not validated for human genomic DNA (gDNA) in solution or human gDNA in biological matrices.	Human gDNA (*for further information see JCTLM DB Cycle 19 (2022) nomination form)*
Measurement range	130 to 70000 copies per 20 µL dPCR reaction	*See JCTLM DB Cycle 19 (2022) nomination form*
Expected uncertainty range	10% to 20% (relative expanded uncertainty)	*See JCTLM DB Cycle 19 (2022) nomination form*

The NML/LGC RMP uses the primers and probes applied initially in digital PCR (dPCR) format by Taly *et al*. (2013). The NIMC RMP also references the method by Taly *et al*. (2013) however there are some minor differences in the primer and probe sequences (Table 2).

Table 2: Comparison of the NML/LGC and NIMC RMP primer and probe sequences

RMP **Oligonucleotide**	**NML/LGC**	**NIMC**
Forward primer	AGGCCTGCTGAAAATGACTGAATAT	GCCTGCTGAAAATGACTGAATATAAACT

Reverse primer	GCTGTATCGTCAAGGCACTCTT	GCTGTATCGTCAAGGCACTCTT
p.G12D probe	FAM-TGGAGCTGATGGCGT-MGB	FAM- TTGGAGCTGATGGCGTA-MGB
WT probe	VIC-TTGGAGCTGGTGGCGT-MGB	VIC-TTGGAGCTGGTGGCGTA-MGB

Oligonucleotide sequences are shown 5' to 3'. Key: Yellow (underlined) indicates bases which are additional to those in the corresponding oligonucleotide used by the other RMP.

The WHO 1st International Reference Panel for genomic *KRAS* codons 12 and 13 mutations material for *KRAS* p.G12D was chosen as the study material based on it containing a *KRAS* p.G12D vAF within the range of the nominated RMP and availability in both the UK and China.

Materials and Methods

Reconstitution of the study material

The WHO 1st International Reference Panel for genomic *KRAS* codons 12 and 13 mutations (NIBSC code: 16/250) consists in eight individually coded ampoules containing lyophilized purified gDNA extracted from human cell lines.

The panel was shipped at room temperature and stored at -20 °C upon arrival. All the ampoules received appeared to be intact and in a good condition.

For this study, only the ampoule containing gDNA carrying the *KRAS* p.G12D (CDS c.35G>A) mutation (NIBSC code: 16/260) was analysed (Table 3).

Table 3. Manufacturer's values for the Study Material (NIBSC 16/260)

Material	*KRAS* codon 12 or 13 mutation	Consensus mutation percentage (%)	Consensus mutant *KRAS* copy number per diploid genome mass	Consensus total *KRAS* copy number per diploid genome mass	Expected mass concentration (ng/µL)
16/260	p.Gly12Asp	71.5	3.09789	4.3482	50 ng/µL

The 16/260 vial was reconstituted gravimetrically following the manufacturer's instructions (NIBSC, 2020). Full details of the gravimetric protocol are given in Appendix 1. After reconstitution, the study material was decanted into a new DNA Lo-bind tube (Eppendorf) and stored at 4 °C until the completion of the analysis (6 days in total).

The concentration of the study material was assessed by fluorometry using Qubit with the dsDNA Broad Range Assay Kit (Invitrogen; Cat No. Q32850, Lot No. 2359061). Three independent 1:10 dilutions were prepared from the material and were each measured in triplicate (total *n*=9). A mean value (± SD) of 45.6 (± 0.6) ng/µL was obtained which was close to the expected value (Table 3).

Serial dilutions of the study material were gravimetrically prepared in 0.1 x Tris-EDTA pH 8.0 (TE) (Sigma BioUltra; Cat No. 93283, Lot No. BCCD5804) to give two dilutions to be analysed by dPCR: dilution "D2" and dilution "D3", nominally 8.0 ng and 1.6 ng/reaction respectively, based on the expected mass concentration (Table 3). These two dilutions were chosen to reduce the number of double positive partitions containing more than one target molecule prior to amplification. This was to minimise the impact of the pseudogene *KRASP1* on the quantification (see next section).

Considerations for experimental design

The human genome contains a *KRAS* pseudogene *KRASP1* (chromosome 12) which has high homology with the *KRAS* gene (chromosome 6) (Figure 1). PCR analysis of human gDNA material with the

NML/LGC dPCR RMP (Whale et al. 2018) is predicted to result in co-amplification of *KRASP1* with detection by the *KRAS* WT probe (due to 100% homology of the probe region). *KRASP1* is expected be amplified with reduced efficiency compared to *KRAS* due to three primer binding mismatches (Figure 1).

```
KRAS        TTATGTGTGACATGTTCTAAT----ATAGTCACATTTTCATTATTTTTATTATAAGGCCT      56
KRASP1      ----GTGGCGCAGGCACTGAAGGCGGCGGCAGGGCCAGAGGCTCAGCGGCTCCCAGACCT      56
                ***   ** *  ** *        *                     *   ** ***

KRAS        GCTGAAAATGACTGAATATAAACTTGTGGTAGTTGGAGCTGGTGGCGTAGGCAAGAGTGC      116
KRASP1      GCTGAAAATGACTGAATATAAACTTGCGGTAGTTGGAGCTGGTGGCGTAAGCAAAAGTGT      116
            ************************* ********************** **** ****

KRAS        CTTGACGATACAGCTAATTCAGAATCATTTTGTGGACGAATATGATCCAACAATAGAGGT      176
KRASP1      CTTGACGATACAGCTAATTCAGAATCATTTTGTGGACCAATATGATCCAACAATAGAGAA      176
            ************************************ ******************

KRAS        AAAT  180
KRASP1      TTCC  180
```

Figure 1: ClustalW alignment of the amplicon of the *KRAS* assay used in the study with ±50 bp and the equivalent sequence of the *KRASP1* pseudogene. The position of the NML/LGC RMP assay is highlighted (yellow, forward primer; green, wild-type probe; cyan, reverse primer).

As all human gDNA samples containing *KRAS* will also contain *KRASP1*, two control materials (gBlocks, Integrated DNA Technologies (IDT)) were designed containing either the *KRAS* target sequence or the homologous *KRASP1* region to assist in the position of the threshold for the analysis (Table 4).

Other control samples that were included in the experiment were commercially available human gDNA ("Promega gDNA") to monitor assay false positive rate (FPR) and a *KRAS* p.G12D 50% vAF reference standard (Horizon Discovery) ("HZN vAF 50%") as a positive control (Table 4). All control samples were diluted to ~ 600 target copies/reaction.

Table 4. Control samples

Short control name	Control name and description	Control purpose	Approximate concentration (copies/reaction)
*KRAS*_WT gBlock	IDT customised gene fragment based on NG_001154.4:172-301	Positive control for WT *KRAS* in the absence of *KRASP1* target molecules. Support the position of the threshold to classify genuine positive *KRAS* WT partitions.	600 WT *KRAS*
KRASP1 gBlock	IDT customised gene fragment based on NG_007524.2:10582-10711	Positive control for *KRASP1* identify the end-point fluorescence of partitions containing the *KRASP1* target.	600 *KRASP1*
Promega gDNA	Human genomic DNA from healthy donors (Promega; Cat No. G304A, Lot No. 0000468220)	Negative (wild-type) control for *KRAS* p.G12D to estimate false positive rate (FPR).	600 WT *KRAS*
HZN vAF 50%	*KRAS* G12D Reference Standard, 50% (Horizon	Positive control for WT and p.G12D *KRAS* of known vAF.	600 WT *KRAS* and 600 G12D *KRAS*

	Discovery; Cat No. HD272, Lot No. 51252)		
NTC H2O	Nuclease-free water (Thermo Fisher Scientific; Cat No. AM9937, Lot No. 2004097)	No template control to check for contaminating targets in the reagents.	0
NTC TE	Tris-EDTA pH 8.0 (TE) (Sigma BioUltra; Cat No. 93283, Lot No. BCCD5804)	No template control to check for contamination targets in the diluent during sample dilution.	0

Digital PCR (dPCR)

Both dilutions (D2 and D3) of the study material and controls were analysed in triplicate in three independent experiments (total *n*=9) following the NML/LGC RMP standard operating procedure (SOP) (see separate document MOLDIGI/SOP-007). This method uses the QX200™ Droplet Digital™ (ddPCR™) PCR system. For each reaction, 8.8 µL of each template was added to a final volume of 22 µL per pre-reaction with 20 µL of this used to prepare droplets.

The data were analysed using the QuantaSoft™ software version 1.7.4.0 (Bio-Rad). The threshold was set using the positive controls as follows. Firstly, the wells containing the *KRASP1* gBlock and the *KRAS*_WT gBlock were selected using the 1D plot for Channel 2 (Ch2) (which detects the WT *KRAS* probe signal). The Ch2 threshold was positioned below the *KRAS* WT-positive partition cluster but above the *KRASP1*-positive partitions to maximise number of WT positive partitions and minimise the number of *KRASP1*-positive droplets. This was repeated for the three different experiments to identify a threshold that was suitable for all the reactions (Figure 2A). The threshold was then applied to the rest of the wells in the three experiments (Figure 2B, Figure 3A-B).

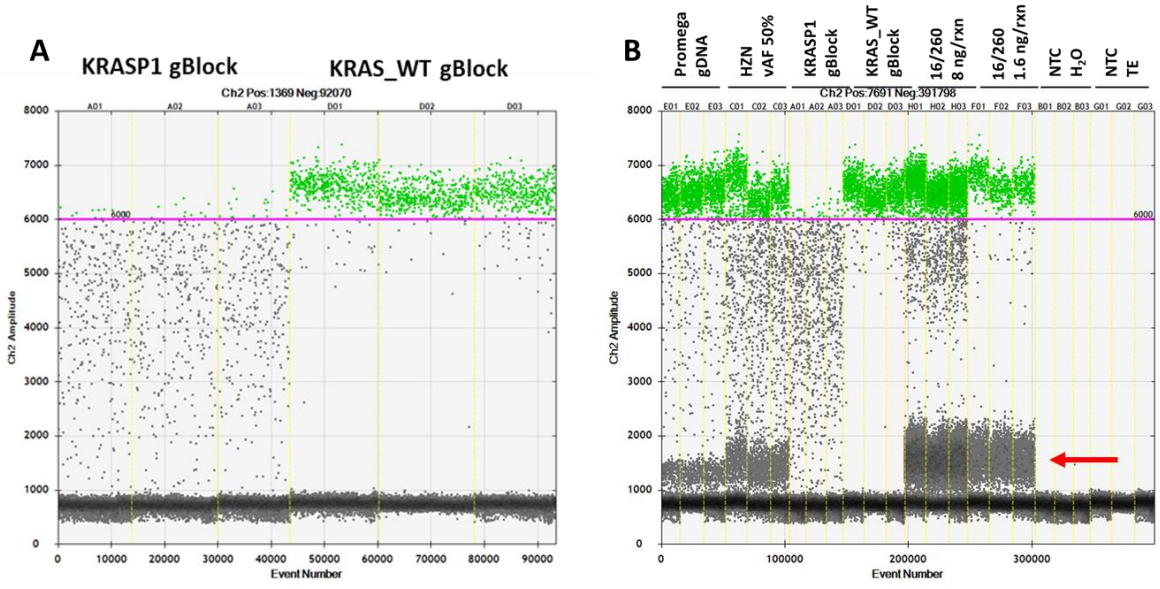

Figure 2. Representative 1-D plots from the QuantaSoft™ software to illustrate how the threshold was manually set for the *KRAS* WT signal. (**A**) Threshold setting in Ch2 1D plot, using signal obtained from reactions containing *KRAS*_WT and *KRASP1* gBlocks as guidance. (**B**) The same threshold (6000) was then applied to all the samples in all three experiments. *Note*. The "rain" observed in the reactions containing human gDNA is likely to be the result of *KRASP1* amplification. The second cluster of partitions in the negative cluster (red arrow) may be due to assay cross-reactivity with other regions of lesser homology (vs. *KRASP1*) within the human genome.

The Channel 1 (Ch1) threshold (for *KRAS* p.G12D detection) was set using HZN 50% vAF positive control (Figure 3C). To account for partition-specific PCR competition that occurs in SNV assays and is observed by a 45° reduction in fluorescent signal of the double positive cluster in both channels (Whale *et al*., 2016), the lasso tool was used to classify the double-positive partitions. The *KRAS* G12D vAF 50% Reference Standard was used to confirm that the position of the threshold was correct by verifying that the *KRAS* p.G12D vAF was close to 50% as expected (Figure 3C). The Promega (wild-type) gDNA control was analysed (Figure 3D) and the *KRAS* p.G12D FPR of the assay (0.03%) was comparable to previous studies (~0.03%; Whale et al., 2018). dPCR 2D plots for study material dilutions D2 and D3 are shown in Figure 3E and 3F, respectively.

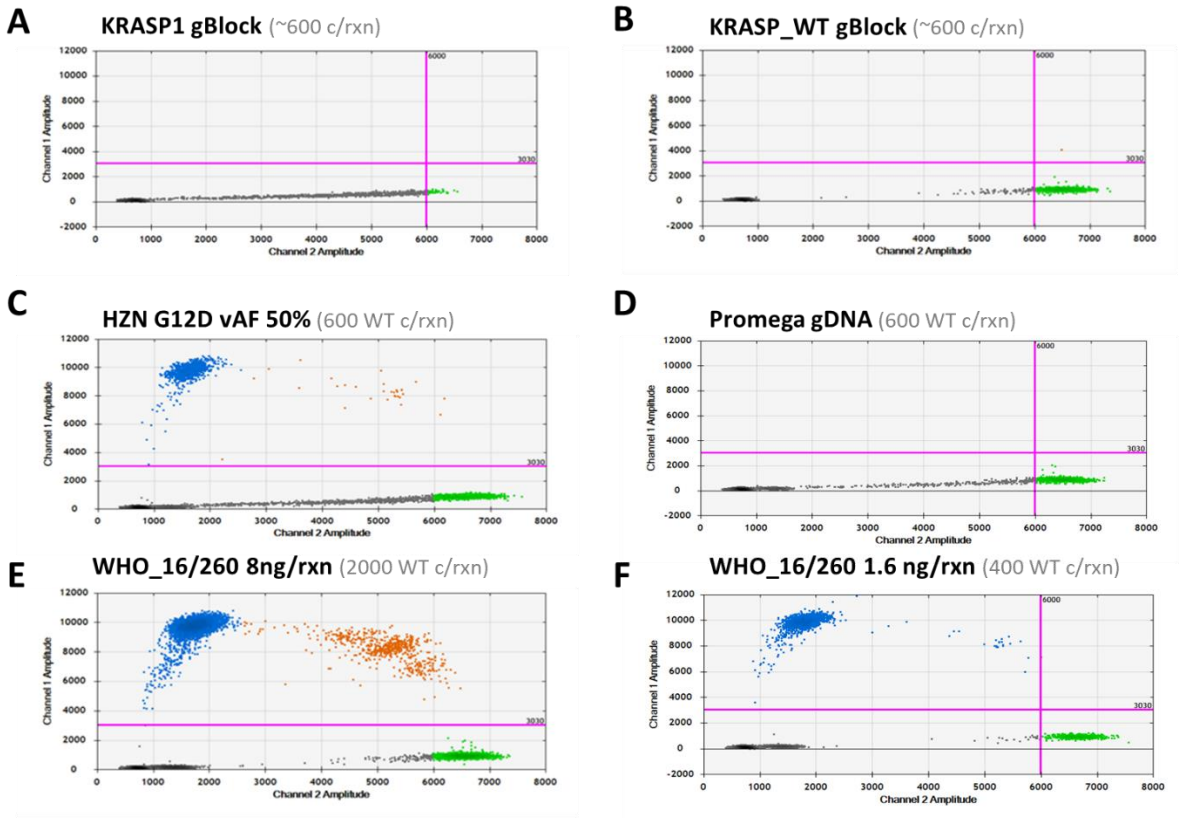

Figure 3. Representative 2D plots from the QuantaSoft™ software for controls and study material. 2D plot of the (**A**) *KRASP1* and (**B**) *KRAS*_WT gBlocks, (**C**) *KRAS* p.G12D Reference Standard (vAF 50%; HZN) , (**D**) Promega wild-type gDNA control, (**E**) D2 and (**F**) D3 of WHO/NIBSC *KRAS* p.G12D material (16/260). In all plots, the Ch1 (horizonal pink line) and Ch2 (vertical pink line) thresholds are set as described in the text. Cluster colour code: black = negative partitions, blue = partitions containing only KRAS G12D, green = partitions containing only KRAS WT and orange = double positive partitions containing both G12D and WT. Lasso correction function not showing for reactions not containing G12D partitions.

Following partition classification, copies per partition (λ) were calculated according to MOLDIGI/SOP-007. Mean λ values for study material D2 and D3 dilutions were 0.189 and 0.039 (*KRAS* p.G12D), and 0.072 and 0.015 (*KRAS* WT). (The validated copy number concentration measurement range of the RMP is $0.004 < \lambda < 3$ which corresponds to 130 to 72,000 molecules per 20 µL reaction).

KRAS p.G12D and WT copy number concentrations of the reconstituted study material were calculated using a partition volume of 0.749 nL (mean value of those reported by Dagata *et al*. 2016, Kosir *et al*. 2017 and Pinheiro *et al*. 2017 for the ddPCR Supermix for Probes without dUTP) and applying the gravimetric dilution factor. *KRAS* p.G12D vAF values were calculated for each well and a mean value calculated.

Study material *KRAS* variant and wild-type copy number concentration values were calculated using the arithmetic mean and uncertainties estimated based on the data for D2 dilution, due to the expected superior precision at the higher concentration, and compared with the data for the D3 dilution for consistency. Measurement precision was calculated as a Type A uncertainty based on 1-way ANOVA analysis. Type A uncertainty was combined with partition volume uncertainty (5.13%), which was based on the SD of published values (Dagata *et al*. 2016, Kosir *et al*. 2017 and Pinheiro *et al*. 2017). Gravimetric dilution uncertainty was not included as it was considered negligible relative to the other uncertainty contributions.

Mean vAF values were calculated for the D2 and D3 dilutions of the study material and measurement uncertainties estimated based on measurement precision (Type A) by 1-way ANOVA analysis. The measurement uncertainties for both dilution levels were compared with the results for the HZN 50% vAF control (Appendix 2); the variability of the D3 dilution was of a more similar magnitude to that of the positive control, therefore the value and uncertainty for sample dilution D3 is reported.

Results

Table 5. WHO/NIBSC *KRAS* p.G12D material (16/260): NML/LGC Reported values and uncertainties

Measurand	**Reported value/uncertainty (units)**
***KRAS* p.G12D concentration**	**(μL^{-1})**
Mean	29600
Standard uncertainty	1579
Coverage factor (k)	3.18
Expanded uncertainty (Relative)	5100 (17%)
***KRAS* WT concentration**	**(μL^{-1})**
Mean	11200
Standard uncertainty	592
Coverage factor (k)	3.18
Expanded uncertainty (Relative)	1900 (17%)
***KRAS* p.G12D vAF**	**(%)**
Mean	72.2
Standard uncertainty	0.54
Coverage factor (k)	4.30
Expanded uncertainty (Relative)	2.4 (3.3%)

Measurement uncertainties were rounded outwards to 2 s.f. Values are shown to the same order of magnitude/d.p. as the expanded uncertainties.

Conclusions

The high homology between the *KRAS* p.G12/G13 genomic region and the *KRASP1* pseudogene is a potential source of interference affecting dPCR assays measuring *KRAS* copy number concentration or vAF in human gDNA. Testing of the NML/LGC RMP with controls for *KRAS* WT and *KRASP1* indicated that the presence of mismatches in the forward and reverse primers to the *KRASP1* sequence leads to reduced PCR amplification efficiency which manifests as a decrease in end-point fluorescence and is observed as “rain” in the signal channel for *KRAS* WT (Figures 1-3). The *KRAS* p.G12D signal does not

appear to suffer from this issue due to the mismatch between the variant-specific probe and the *KRASP1* sequence (Figure 3A). By applying synthetic controls for *KRAS* WT and *KRASP1*, we were able to set thresholds to reduce the misclassification of putative *KRASP1*-containing droplets, which would lead to overestimation of *KRAS* WT copy number concentration and underestimation of *KRAS* p.G12D vAF. However, the lack of clearly separated dPCR clusters for *KRASP1*- and *KRAS*-containing partitions, combined with the possibility of partitions which contain both *KRAS* and *KRASP1* template (especially at higher lambda values) which would also lead to 'rain', are challenges in the application of this assay to human gDNA templates.

We observed more Ch2 'rain' for the HZN 50% vAF and Promega wild-type gDNA controls compared to the study material (Figure 3). This may be due to the higher *KRAS* copy number per diploid genome in the study material (Table 3). Alternatively, the copy number or sequence of *KRASP1* may vary between materials.

Performance of the NML/LGC RMP was within the expected uncertainty range for *KRAS* p.G12D and WT copy number concentration measurements when applied to the study material. As vAF measurements are not within the current scope of the NML/LGC RMP, measurement uncertainty of the study material vAF was reported conservatively based on performance of controls and previous results (Whale et al 2018).

References

Dong L, *et al*., (2018), 'Evaluation of droplet digital PCR and next generation sequencing for characterizing DNA reference material for *KRAS* mutation detection'. Sci. Rep. 8:9650.

Dagata JA, Farkas N, Kramar JA (2016), 'Method for Measuring the Volume of Nominally 100 µm Diameter Spherical Water-in-Oil Emulsion Droplets'. NIST Special Publication 260-184.

Kosir AB, *et al*. (2017), 'Droplet volume variability as a critical factor for accuracy of absolute quantification using droplet digital PCR'. Anal. Bioanal. Chem. 409 (28): 6689-97.

MOLDIGI/SOP-007 LGC primary reference measurement procedure for *KRAS* G12D and wild-type in solution using digital PCR (Issue 1, dated 29 May 2018)

NIBSC code: 16/250 Instructions for use (Version 3.0, Dated 16/03/2020). WHO Reference Panel: 1st International Reference Panel for genomic *KRAS* codons 12 and 13 mutations.

Pinheiro LB, *et al*. (2017), 'Interlaboratory Reproducibility of Droplet Digital Polymerase Chain Reaction Using a New DNA Reference Material Format'. Anal. Chem. 89 (21): 11243-11251.

Taly V, *et al*. (2013), 'Multiplex picodroplet digital PCR to detect *KR*AS mutations in circulating DNA from the plasma of colorectal cancer patients'. Clin. Chem.59: 1722–31.

Whale AS, *et al*., (2018), 'Assessment of Digital PCR as a Primary Reference Measurement Procedure to Support Advances in Precision Medicine'. Clin. Chem. 64 (9): 1296–1307.

Whale AS, *et al*., (2016), 'Fundamentals of multiplexing with digital PCR'. Biomol Detect Quantif. 10: 15-23.

Appendix 1: Gravimetric reconstitution and dilution of the study material

Gravimetric reconstitution and dilution were performed using an analytical balance (Mettler; MT5, serial No: N20555) calibrated with OIML F1 Class weights (Zwiebel; No CE: Z2218092, serial No. S2218092; wire weights, range of 1 mg – 500 mg).

The vial of study material (NIBSC 16/260) was gently tapped to collect the lyophilized at the bottom.

The ampoule was opened, and the weight of the ampoule's body containing the freeze-dried gDNA was registered (w1). Nuclease-free water (100 µL) was added (Thermo Fisher Scientific; Catalog No. AM9937, Lot No. 2004097) and the weight was registered (w2).

The reconstituted material was transferred to a DNA LoBind® nuclease free tube (Eppendorf).

The reconstituted material was incubated for 1 hour at room temperature and homogenised by pipetting.

The mass of the reconstitution volume was calculated by subtracting the mass of the ampoule containing only the lyophilized (w1) from the mass of the reconstituted vial (w2) being 100.08 mg.

Gravimetric dilution to ~ 1 ng/µL and 0.2 ng/µL was performed by recording the following weight (w) measurements:

- Empty tube (w1)
- Tube after adding the diluent (w2)
- Tube after adding the sample (w3)

The following calculations were made:

$$Mass\ of\ the\ diluent\ = w2 - w1$$

$$Mass\ of\ the\ sample = w3 - w2$$

$$Gravimetrical\ dilution\ factor\ (GDF) = \frac{(mass\ of\ the\ diluent + mass\ of\ the\ sample)}{mass\ of\ the\ sample}$$

Then, the GDF was used to calculate the concentration of the stock.

Appendix 2: Software vAF plots from all experiments

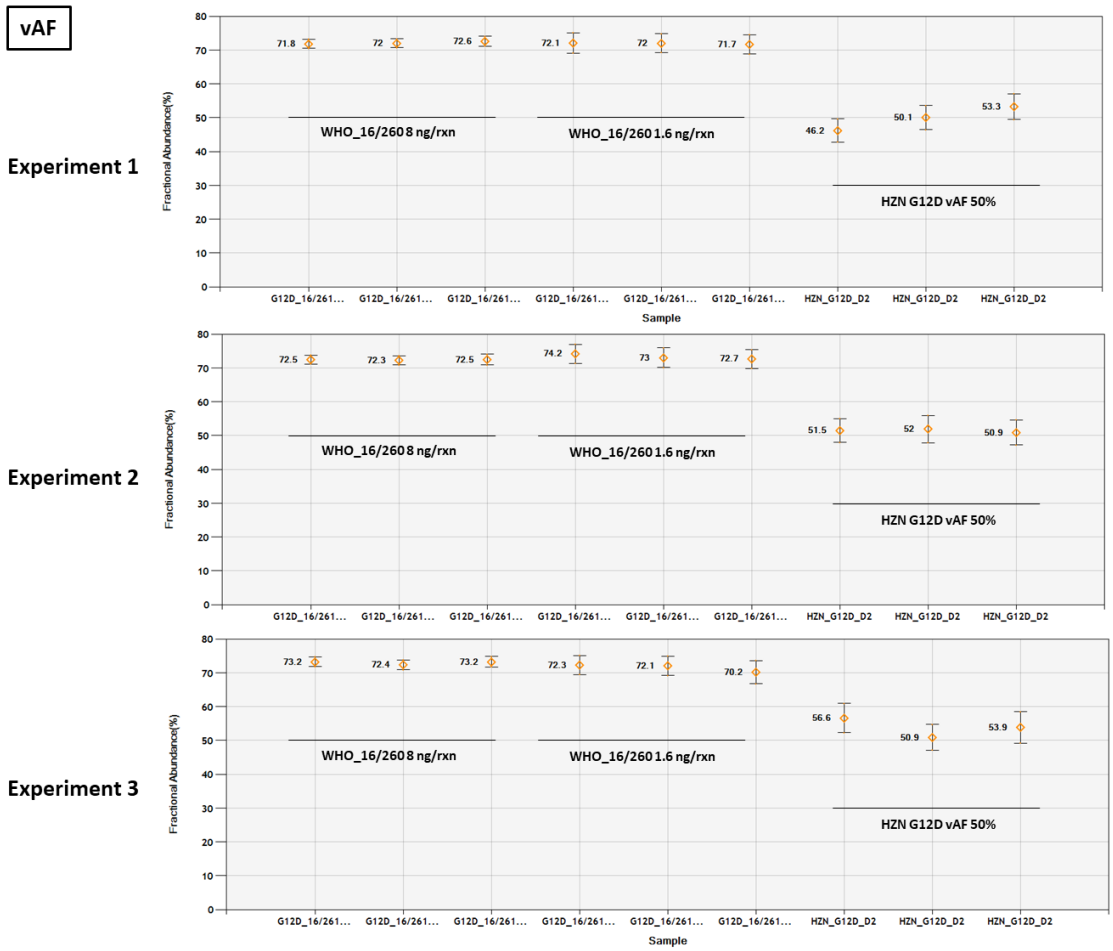

Figure A1. vAF of the WHO_16/260 samples and the HZN *KRAS* p.G12D vAF: 50% Reference Standard. Single measurements with theoretical (Poisson) error (95% confidence intervals) are shown for each experiment.